

Supporting Information

to

Counterion-Mediated Hierarchical Self-Assembly of an ABC Miktoarm Star Terpolymer

*By Andreas Hanisch, André H. Gröschel, Melanie Förtsch, Markus Drechsler, Hiroshi Jinnai,
Thomas M. Ruhland, Felix H. Schacher,* and Axel H. E. Müller**

Table of Contents

1. Additional Experimental Section.....	p. 2
2. Synthesis and Characterization of PB- <i>arm</i> -P2VP- <i>arm</i> -PtBMA Miktoarm Star Ter- polymer.....	p. 5
3. Self-Assembly of μ -BVqT.....	p. 7
3.1. Intermediate Structures of “Woodlouse” Aggregates.....	p. 9
3.2. Importance of the Nature of the Counterion.....	p. 12
3.3. Structural Characterization of “Woodlouse” Aggregates.....	p. 14
References.....	p. 16

1. Additional Experimental Section

Synthesis

Quaternization of 2-vinylpyridine homopolymers (P2VP) and preparation of aqueous solutions

The quaternization procedure was similar to the method described for the miktoarm star terpolymer with slight modifications. After three days of reaction with methyl iodide 10 vol% of water were added to the partially precipitated reaction mixture in dioxane and it was allowed to stir for an additional day. Afterward, it was first dialyzed to a mixture of dioxane:water (90:10) and then the solvent composition was gradually increased to (80:20). The obtained stock solution in the dioxane:water mixture was afterward dialyzed to water. The triiodide complexes were prepared in the same manner as described in the manuscript.

Preparation of μ -BVqT with different counterions

The exchange of the iodide counter ion with chloride was achieved by dialysis of the dioxane stock solution to 50 mM solution of LiCl in THF. Afterward the solution was dialyzed against pure THF to remove excess salt. Before dialysis to water, the solvent was again changed to dioxane through dialysis.

The quaternizations with dimethyl sulfate were conducted either in THF or dioxane. A polymer solution was prepared with a concentration of 2 g/L and then degassed for 15 minutes. Afterward, 10 equiv of dimethyl sulfate regarding 2VP units were added and the reaction mixture was allowed to stir at 40 °C for 3 days. Finally the solution was purified from the excess quaternization agent by dialysis with the respective reaction medium. After dilution to a concentration of 1 g/L the solutions were dialyzed to water.

Characterization

Size Exclusion Chromatography (SEC)

SEC measurements were performed on a set of 30 cm SDV-gel columns (5 μ m bead size, with pore sizes of 10^5 , 10^4 , 10^3 and 10^2 Å) using refractive index and UV (λ = 254 nm) detection. THF was used as eluent at a flow rate of 1 mL/min. Toluene was used as internal standard

and the system was calibrated with PS and 1,4-PB standards

¹H NMR spectroscopy

¹H NMR spectra were recorded on a Bruker Ultrashield 300 spectrometer at an operating frequency of 300 MHz. CDCl₃ was used as solvent and tetramethylsilane as internal standard.

Matrix-Assisted Laser Desorption Ionization Time-of-Flight Mass Spectrometry (MALDI-ToF MS)

MALDI-ToF MS analysis was performed on a Bruker-Reflex III apparatus equipped with a N₂ laser ($\lambda = 337$ nm) at an acceleration voltage of 20 kV. *trans*-2-[3-(4-*tert*-Butylphenyl)-2-methyl-2-propenylidene]malonitrile (DCTB, Fluka, 99,0 %) was used as matrix and silver trifluoroacetate (AgTFA, Sigma-Aldrich, 99.99%) as ionization agent. Samples were prepared from THF solution by mixing matrix, polymer and salt in a ratio of 20/5/1 (v/v).

Scanning Electron Microscopy (SEM)

The particles were analyzed by field emission scanning electron microscopy on a Zeiss LEO 1530 Gemini microscope equipped with a field emission cathode operating at 0.5-5 kV. Specimen preparation was accomplished as follows: silicon wafers were cleaned using isopropanol and acetone in a standard procedure. To obtain areas of different concentration of particles, the wafer was first dip-coated from 0.02 g/L solution and then a further drop of the solution was deposited and allowed to dry. The specimens were coated with a thin platinum layer using a sputter coater (Cressington 208HR) to render the specimen conductive.

Dynamic Light Scattering (DLS)

DLS measurements were performed on an ALV DLS/SLS-SP 5022F compact goniometer system with an ALV 5000/E cross correlator and a He-Ne laser ($\lambda = 632.8$ nm). The measurements were carried out in cylindrical scattering cells ($d = 10$ mm) at an angle of 90° and a temperature of 20 °C. Prior to the light scattering measurements, the sample solutions were filtered using nylon filters (Magna, Roth) with a pore size of 5 μ m. The CONTIN algorithm was applied to analyze the obtained correlation functions. Apparent

hydrodynamic radii were calculated according to the Stokes-Einstein equation.

DSC

Thermal analysis and determination of the glass transition temperatures was performed on a Perkin–Elmer Diamond DSC at a heating rate of 20 K/min.

2. Synthesis and Characterization of PB-*arm*-P2VP-*arm*-PtBMA Miktoarm Star Terpolymer

The synthesis of the PB-*arm*-P2VP-*arm*-PtBMA miktoarm star terpolymer was accomplished by combining sequential anionic polymerization with azide-alkyne Huisgen cycloaddition. Therefore, an alkyne-functionalized polybutadiene-*b*-poly(2-vinylpyridine) (PB-*b*-P2VP) diblock copolymer was directly prepared by anionic polymerization using an alkyne-functionalized DPE derivative (click-DPE). The molecular characterization of the diblock copolymer is listed in **Table 1**. As already reported, in the case of the click-DPE, incorporation in, or most probably at the end of the poly(2-vinylpyridine) (P2VP) block takes place. This leads to diblock copolymers which bear additional alkyne-functions in or at the end of the P2VP block, as the DPE derivative is used in excess. Nevertheless, under appropriate reaction conditions, i.e. using only a slight excess of click-DPE, low temperatures and short reaction times an overall degree of alkyne-functionalization of 116 % was achieved.¹ Taking into account the errors of the determination method this resembles only a slight over-incorporation of click-DPE into the material.

The alkyne group is then used to attach the third block, poly(*tert*-butyl methacrylate) (PtBMA), *via* azide-alkyne Huisgen cycloaddition. Thus, in the following click reaction an excess of 10% of azido-functionalized homopolymer chains relative to the diblock chains was used to ensure that all diblock chains undergo conjugation. As a direct consequence the obtained miktoarm star terpolymer contains a minor fraction with more than one chain of PtBMA. **Figure S1** displays the SEC traces of the precursor homopolymer and diblock copolymer, and the obtained miktoarm star terpolymer. **Table 1** lists the corresponding characterization data. Due to the use of an azido-functionalized ATRP initiator for the PtBMA polymerization in case of recombination polymers bearing two azido end-groups are formed. Therefore, a small percentage of α,ω -azido-bifunctionalized homopolymer could lead to H-shaped miktoarm star terpolymers and explain the observed higher molecular weight shoulder. From test click reactions with PS homopolymers, where the bromo-function was transformed into an azide after polymerization, no such coupling shoulder was detected, supporting our assumption.

Table 1. Molecular characteristics of poly(*tert*-butyl methacrylate) (T), polybutadiene-*block*-poly(2-vinylpyridine) (BV), and μ -BVT.

Polymer ^a	M_n^b / kg/mol	PDI ^c
T ₅₃	7.6	1.17
B ₁₀₉ V ₈₁	14.7	1.02
μ -B ₁₀₉ V ₈₁ T ₅₃	22.2	1.07

^aThe subscripts denote the degrees of polymerization of the corresponding blocks as calculated from the respective number average molecular weights. ^bFor the PtBMA homopolymer the number average molecular weight was determined by SEC using a PtBMA calibration. For the diblock copolymer the molecular weight was calculated from ¹H NMR using the molecular weight of the PB as reference. This was measured directly *via* MALDI-ToF MS. For the ABC miktoarm star terpolymer the overall molecular weight was calculated from the corresponding precursor polymers. ^cDetermined by SEC in THF calibrated with PS standards or in the case of PtBMA homopolymer with PtBMA standards.

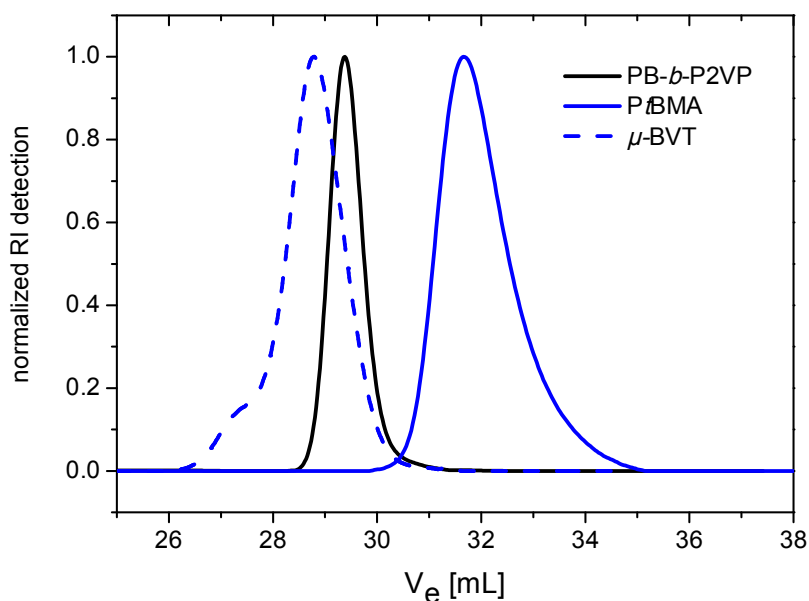


Figure S1. SEC eluograms of the PB-*arm*-P2VP-*arm*-PtBMA miktoarm star terpolymer (μ -BVT), the precursor diblock copolymer (PB-*b*-P2VP), and the homopolymer (PtBMA). In all cases the RI signal is shown.

3. Self-Assembly of μ -BVqT

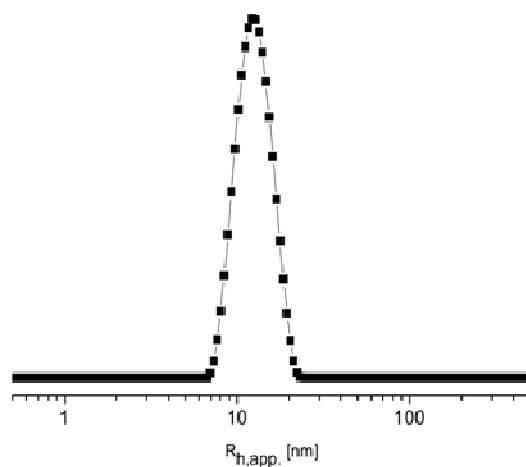


Figure S2. Intensity-weighted DLS CONTIN plot (A) of quaternized μ -BVT (μ -BVqT) in 1 g/L dioxane solution, $R_{h,app} = 12.5$ nm.

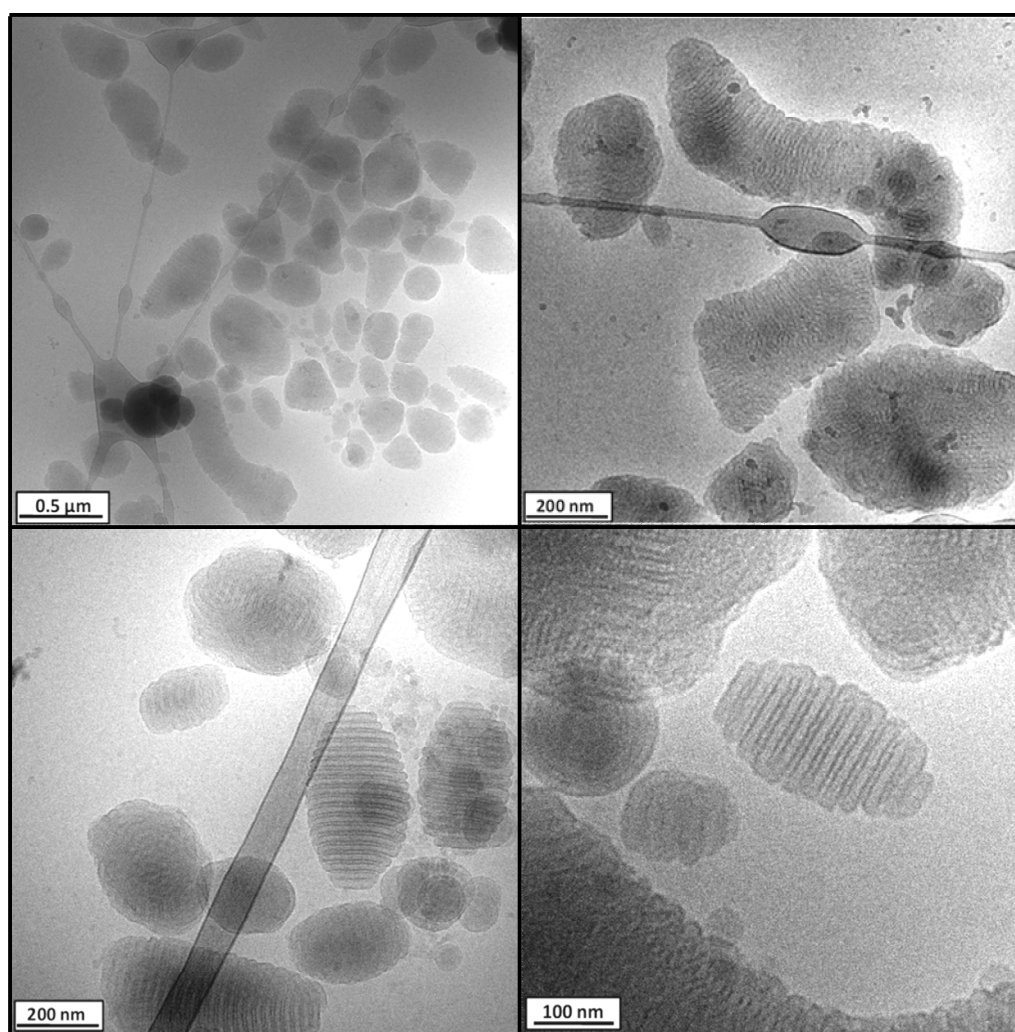


Figure S3. Overview of various cryo-TEM images of different “woodlouse” aggregation forms observed in ~ 0.6 g/L aqueous solutions of μ -BVqT.

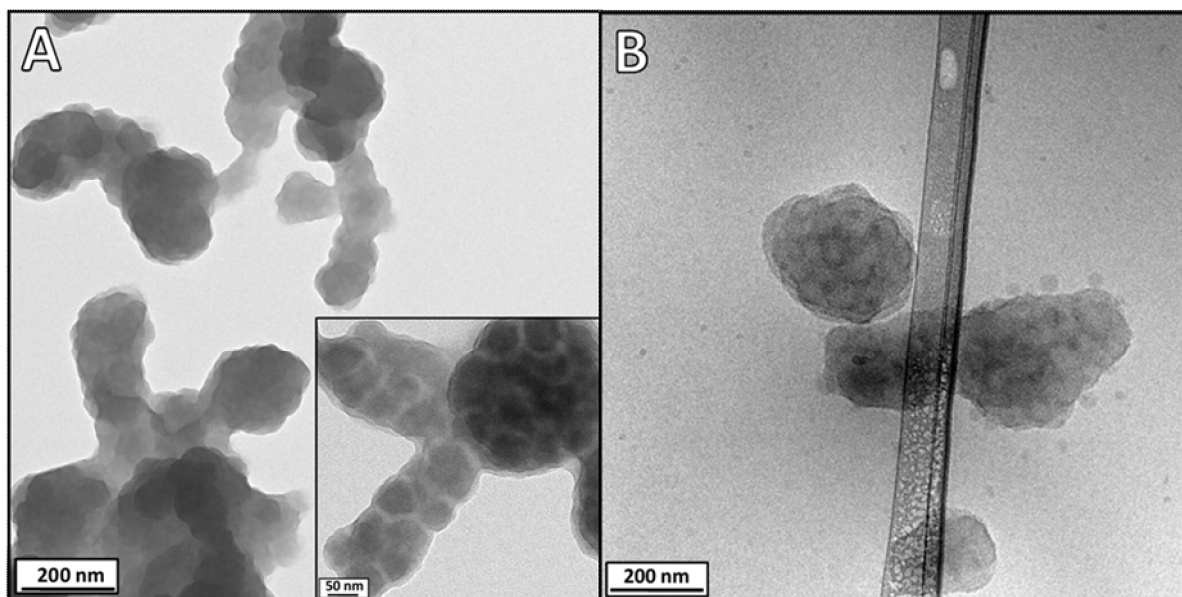


Figure S4. (A) TEM and (B) cryo-TEM micrographs from aqueous solutions of linear $B_{1108}Vq_{142}T_{93}$ at 0.2 and 0.65 g/L, respectively. After dialysis to water precipitation occurred gradually. Whereas the image in (A) is unstained, the inset in (A) shows an enlarged area after staining with OsO_4 . In both cases micellar clusters can be seen, without any internal fine structure (see staining in the inset in (A) or the brighter areas in the cryo-TEM in (B)). Please note that the molecular weight of the triblock terpolymer was much higher and also the molar fractions were different to the studied miktoarm star terpolymer μ - $B_{101}V_{81}T_{53}$. Additionally, the sequence was PB - b - $P2VP$ - b - $PtBMA$ due to the restrictions of anionic polymerization and therefore the middle block forms the corona. This leads to a folding of the polymer chain to shield the hydrophobic end blocks.

3.1. Intermediate Structures of “Woodlouse” Aggregates

The dioxane solution of μ -BVqT, which yielded the intermediate structures (Figure 2), was allowed to age for an additional month before dialysis to water. TEM analysis showed that the obtained aggregates were of slightly higher structural order and the internal fine structure of the “woodlouse” was already visible for some objects (Figure S5A). Nevertheless, the structures seem to be kinetically trapped during the process, as further ageing of aqueous solutions did not lead to any increase in order. As observed by cryo-TEM the superstructures were more densely packed (Figure S5B). Less cylindrical protrusions emanate from the center of the aggregates, and the grey-scale analysis confirms three periodic distances ($d_1 = 4.5 \pm 1.0$ nm, $d_2 = 4.5 \pm 1.0$ nm, $d_3 = 9.0 \pm 1.0$ nm). The structure was further visualized using different tilt angles in cryo-TEM (Supporting videos S1 and S2), confirming a 3-dimensional array of the cylinders.

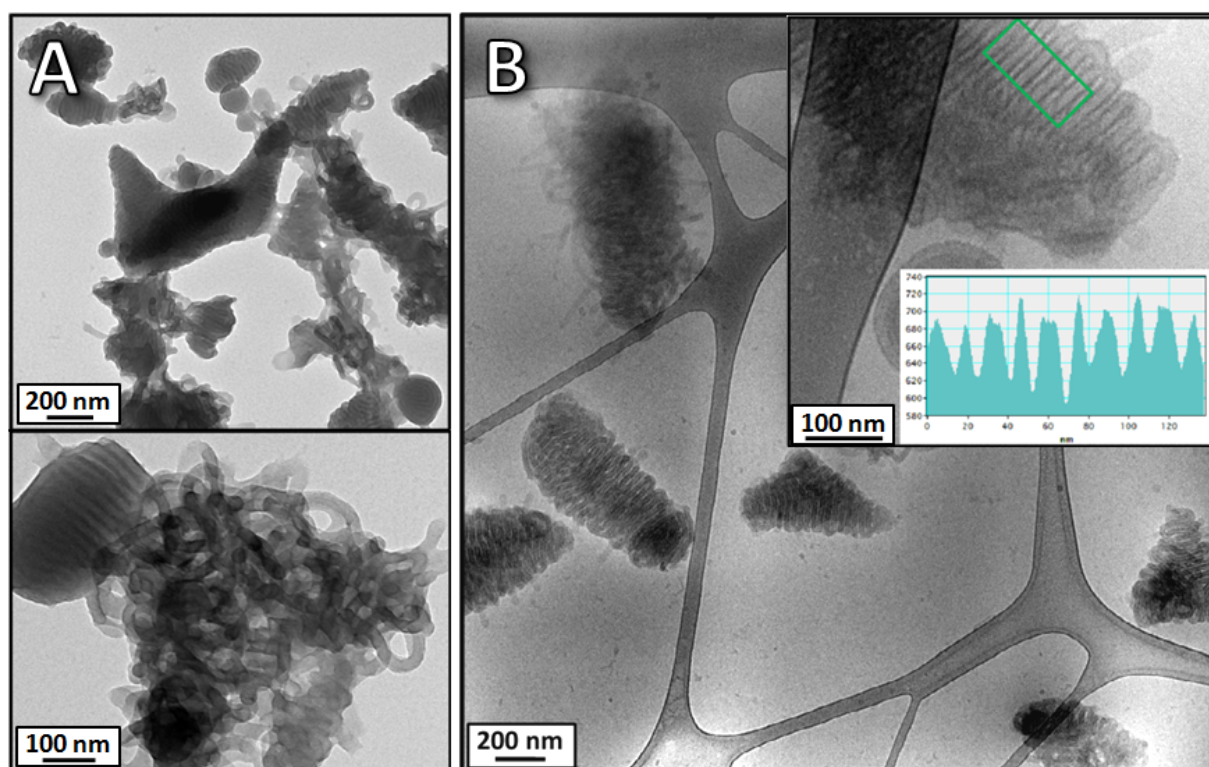


Figure S5. TEM (A) and cryo-TEM micrographs (B) of intermediate micellar structures of μ -BVqT obtained by dialysis to water after ageing of the dioxane solution for one month. The final polymer concentration was 0.2 g/L for TEM and 0.4 g/L in case of cryo-TEM. The upper inset in (B) displays a grey-scale analysis of the highlighted area.

We further prepared thin film cuts of this structural intermediate by freeze-drying of the solution and embedding the particles into an epoxy resin. The corresponding TEM micrographs from thin slices (with and without additional OsO_4 staining) are shown in **Figure S6** and an internal lamellar structure can be observed (black arrows in **Figure S6**). Additionally, OsO_4 staining revealed an undulated shape of the lamellae, which can also be interpreted as a dense packing of spheres (**Figure S6B**). The same observation was made for some of the cylindrical structures (white arrows in **Figure S6B**). As indicated by the white arrows for the non-stained micrographs in **Figure S6A** (only P2VPq is visible), cylindrical protrusions with a tubular nature were also identified. These findings confirm our initial assumption of cylindrical micelles as intermediates. Furthermore, the absence of structures with a diffuse core region supports the assumption of compact particles. The presence of both cylindrical protrusions and elongated particles of rather compact shape with a spherical cross section were further confirmed *via* SEM measurements (**Figure S7**).

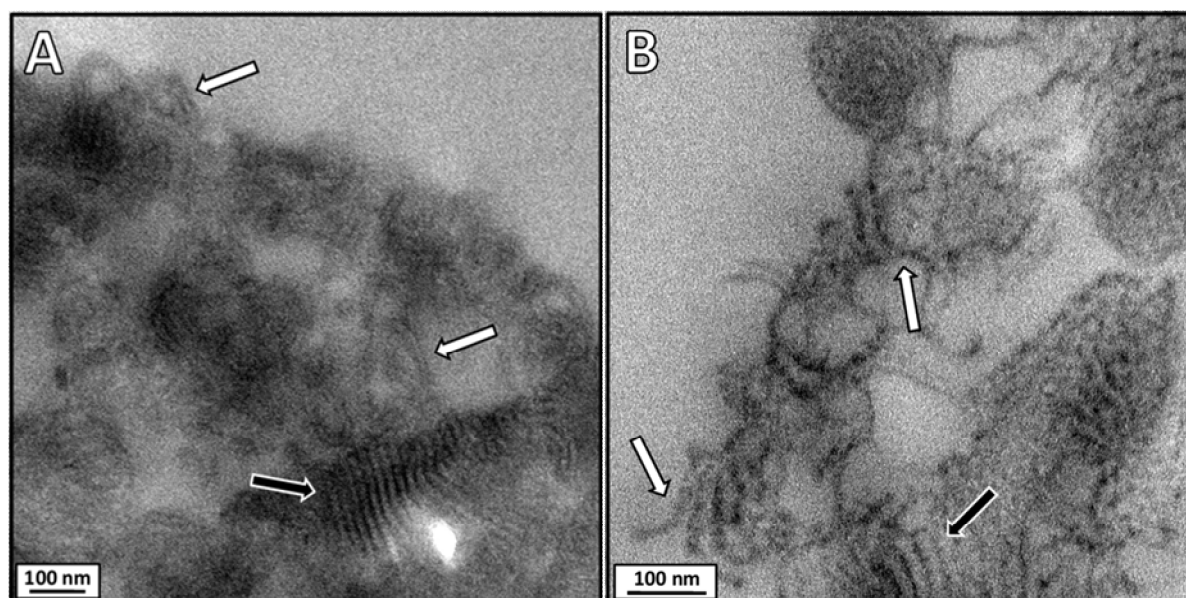


Figure S6. TEM micrographs of 50 nm thick cuts from freeze dried and resin embedded samples of the intermediate structures. This was obtained from the sample depicted in **Figure S5**. The micrograph (A) is unstained, whereas for (B) staining with OsO_4 was performed. The black arrows indicate areas where the lamellar structure of the more densely packed particles could be observed, whereas the white arrows highlight spots, where the cylindrical building units are clearly evident.

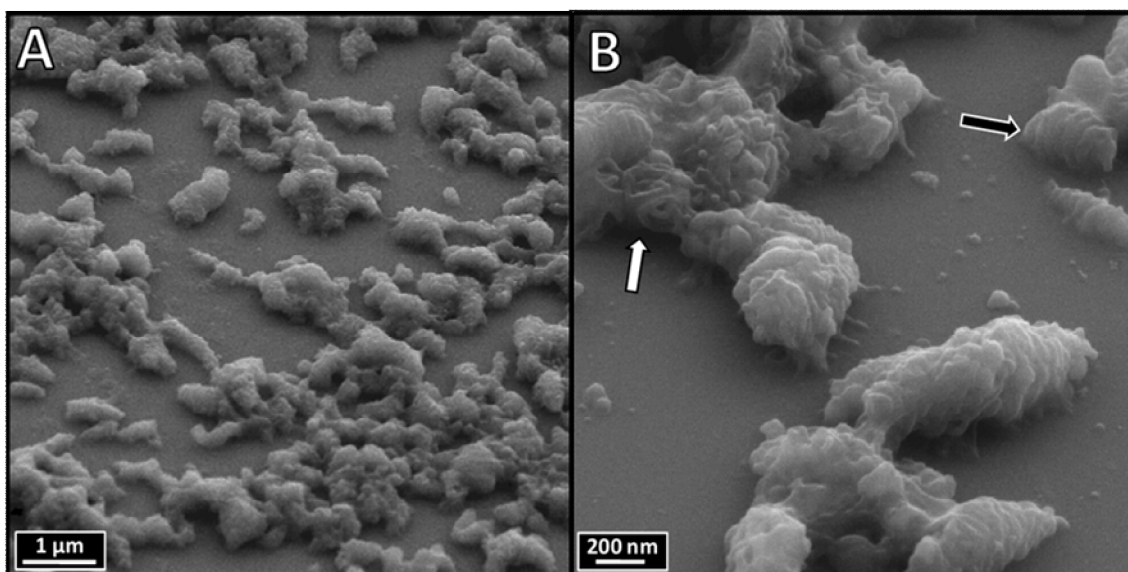


Figure S7. SEM images of intermediate structures obtained from aqueous solutions of μ -BVqT ($c = 0.02$ g/L). The samples were measured on a tilted stage. An irregular array of cylinders is present within the sample. The sample was prepared by dialysis of a quaternized dioxane solution, which was allowed to age for 1 month. Besides ill shaped aggregates (white arrow in B) also some more defined structures are present in the sample (black arrow in B).

3.2. Importance of the Nature the Counterion

To screen the influence of iodine on Poly(*N*-methyl-2-vinylpyridinium iodide), different amounts were added to a homopolymer solution in dioxane/water mixtures as reference system. Subsequent dialysis to water, followed by DLS measurements (Figure S8) revealed the formation of aggregates already for the sample without additional iodine. We attribute this to incomplete quaternization due to the decreasing solubility of P2VPq during the reaction.² However, with additional iodine an increase of the hydrodynamic radii can be clearly observed. Therefore, we assume that the so-formed triiodide counterion leads to a decreased hydrophilicity of the P2VPq segment, inducing further aggregation.

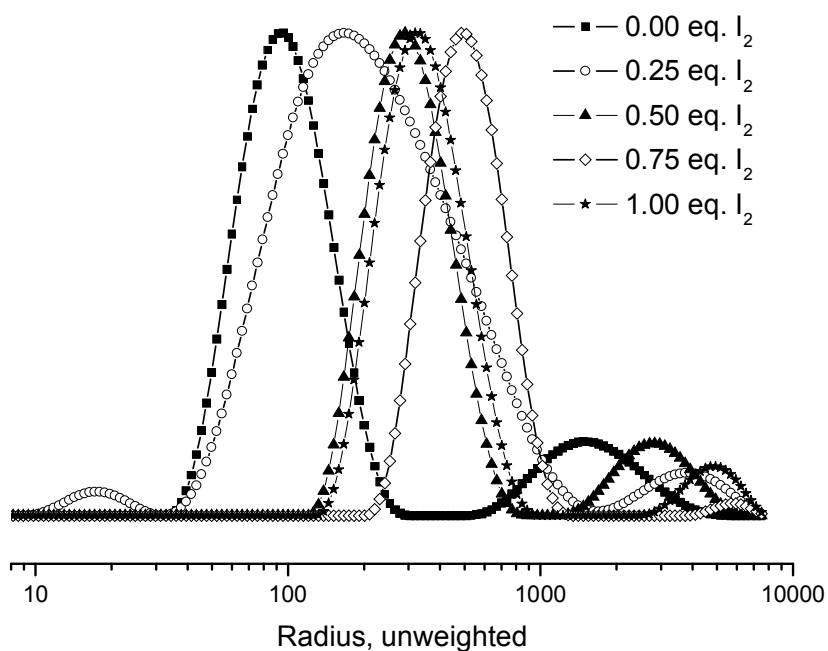


Figure S8. DLS CONTIN plots of solutions of linear P2VPq dialyzed from dioxane:water (80:20) mixtures with different amounts of additional iodine with respect to 2VP monomer units to water. The polymer concentration was ~ 0.4 g/L.

To further substantiate the necessity of iodide as counterion for our system to form triiodide, reference solutions of quaternized μ -BVT with chloride or methyl sulfate as counterions were prepared. In the first case, the dioxane solution of μ -BVqT was dialyzed against a 50 mM solution of LiCl in THF. Subsequent dialysis to water only yielded ill-defined

micellar clusters. When the miktoarm star terpolymer was directly quaternized with dimethyl sulfate, the solution precipitated during the dialysis step to water, both from dioxane and THF solution.

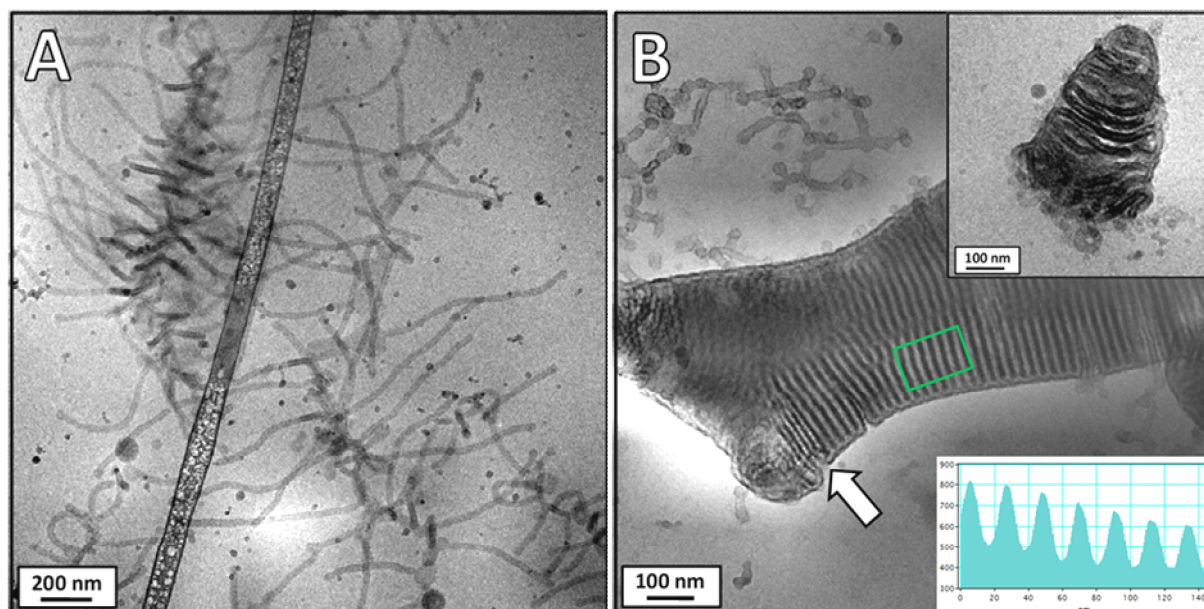


Figure S9. cryo-TEM micrograph of cylindrical aggregates obtained from a micellar solution of μ -BVqT to which 0.08 (A) and 0.42 (B) equiv of iodine were added before dialysis to water. The polymer concentration was ~ 0.4 g/L. The white arrow in B indicates an area, where the lamellae are less densely packed.

3.3. Structural Characterization of “Woodlouse” Aggregates

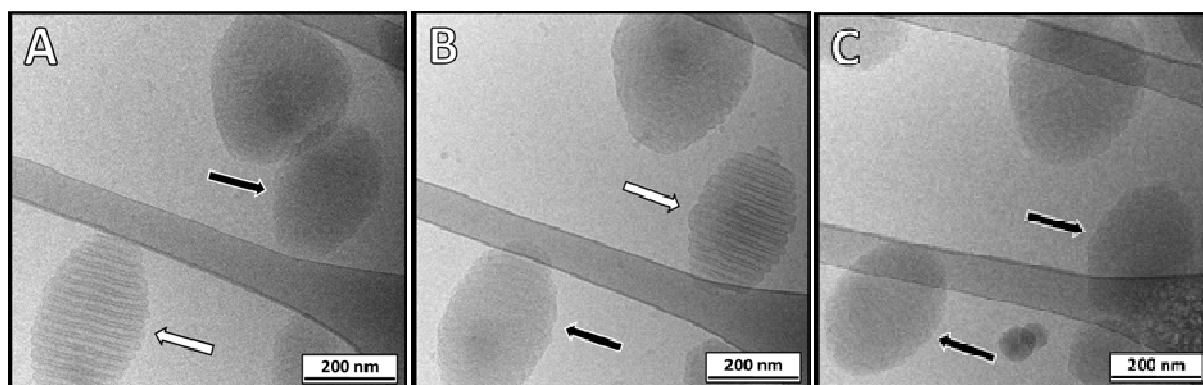


Figure S10. Cryo-TEM micrograph tilt series of an aqueous solution of the “woodlouse” structure (0.6 g/L, μ -BVqT) at 30° (A), 0° (B) and -30° (C) angle. The internal fine structure of the aggregate is only visible, when the longitudinal axis of the object is exactly perpendicular to the direction of the electron beam, as indicated by the white arrows. During tilting the sample the objects leave this optimum position and the fine structure is not visible any more (black arrows).

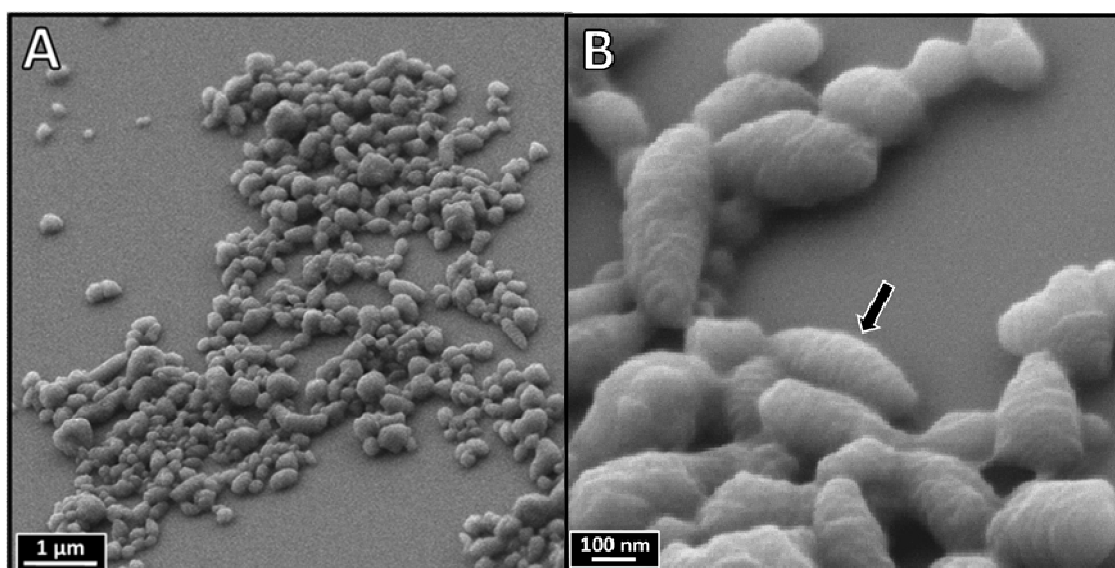


Figure S11. SEM images of “woodlouse”-structured aggregates of μ -BVqT at $c = 0.02$ g/L measured on a tilted sample stage. This allows gaining more information about the depth profile of the structure. The aggregates are not flattened on the surface and retain their circular cross section and 3-dimensional shape as assumed from TEM-tomography. This also supports the assumption of compact non hollow particles. Second, at appropriate angles for some particles a regularly corrugated surface profile was observed (see black arrow in B). This is a direct consequence of the regularly belted structure as detected with TEM/cryo-TEM.

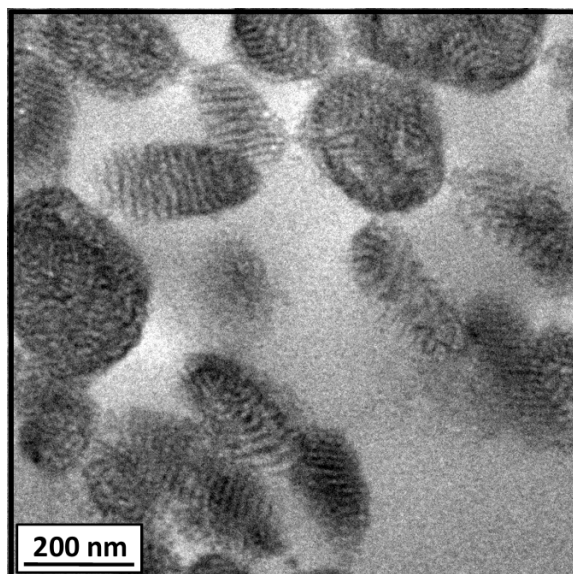


Figure S12. Unstained TEM micrograph of a 50 nm thick cut from a freeze-dried and embedded sample of μ -BVqT aggregates.

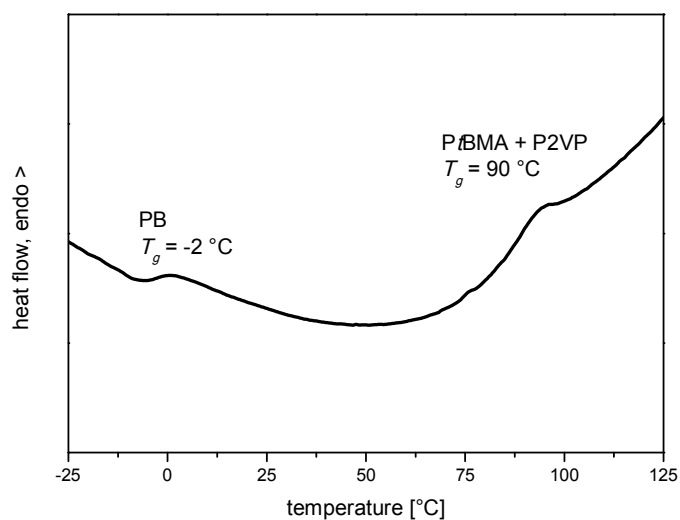


Figure S13. DSC plot for the second heating scan of μ -BVT. The T_g of the polybutadiene precursor homopolymer was determined to be -8.5 °C (not shown). For the miktoarm star terpolymers the transition at -2 °C corresponds to the T_g of the polybutadiene phase, therefore indicating that ligation leads to an increase in T_g . The transition at 90 °C resembles the T_g of PtBMA and P2VP. Similar to literature we attribute this to consist of two nonresolved peaks.³

References

- (1) Hanisch, A.; Schmalz, H.; Müller, A. H. E. A Modular Route for the Synthesis of ABC Miktoarm Star Terpolymers *via* a New Alkyne-Substituted Diphenylethylene Derivative. *Macromolecules* **2012**, *45*, 8300-8309.
- (2) Schacher, F.; Walther, A.; Müller, A. H. E. Dynamic Multicompartment-Core Micelles in Aqueous Media. *Langmuir* **2009**, *25*, 10962-10969.
- (3) du Sart, G. G.; Rachmawati, R.; Voet, V.; van Ekenstein, G. A.; Polushkin, E.; ten Brinke, G.; Loos, K. Poly(*tert*-butyl methacrylate-*b*-styrene-*b*-4-vinylpyridine) Triblock Copolymers: Synthesis, Interactions, and Self-Assembly. *Macromolecules* **2008**, *41*, 6393-6399.